DOI 10.1007/s11182-015-0387-y

Russian Physics Journal, Vol. 57, No. 10, February, 2015 (Russian Original No. 10, October, 2014)

PHYSICS OF MAGNETIC PHENOMENA

INVESTIGATION OF THE COMPOSITION AND ELECTROMAGNETIC PROPERTIES OF LITHIUM FERRITE $LiFe_5O_8$ CERAMICS SYNTHESIZED FROM ULTRADISPERSE IRON OXIDE

A. P. Surzhikov, E. N. Lysenko, A. V. Malyshev, E. V. Nikolaev, S. P. Zhuravkov, and V. A. Vlasov

UDC 621.355

Structural, magnetic, and electric characteristics of $LiFe_5O_8$ *synthesized from ultradisperse iron oxide powder are investigated. The basic* Fe_2O_3 *reagent is prepared by oxidation of iron nanopowder with particle sizes of 100 nm synthesized by the electroexplosive method. It is demonstrated that* $LiFe_5O_8$ *is characterized by fine-grained ceramic structure with average grain size of 1.4 μm, high values of the Curie temperature (~630°C), specific electrical resistance (10^7 Ω·cm), and saturation magnetization (>3300 G). Thus, lithium ferrite so obtained without additives has the parameters suitable for its application as a microwave ferrite material. It is also demonstrated that addition of bismuth ferrite to the lithium ferrite composition during its sintering yields lower values of the specific electrical resistance and relatively high values of the density and saturation magnetization.*

Keywords: lithium ferrite, $LiFe_5O_8$, ceramics, ultradisperse iron oxide, microwave properties, electromagnetic properties.

INTRODUCTION

Lithium ferrites synthesized from $LiFe_5O_8$ are the main functional materials of modern microwave electronics [1]. In addition, these compounds can be used as a cathode material in lithium-ion batteries [2] and in manufacture of sensor elements for gas sensors [3].

The following main requirements are imposed on ferrites intended for operation in the microwave range: high electrical resistance providing small dielectric losses in the material, temperature stability determined by the Curie temperature of the material, and a preset value of the saturation magnetization. From all ferrites, lithium ferrite $LiFe_5O_8$ without additives has the highest Curie temperature and high degree of saturation magnetization. To improve the dielectric and magnetic properties, Ti, Zn, Mn, Co, and Bi are added to the ferrite composition. This deteriorates some ferrite characteristics, primarily, the Curie temperature.

The application of lithium ferrites in microwave techniques imposes high requirements not only on the electromagnetic ferrite parameters, but also on the microstructure of the material that should be uniform throughout the entire volume of a single product and identical for a production lot. Thus, creation of an optimal ferrite microstructure that allows ferrites with required complex of properties to be synthesized is of great importance.

National Research Tomsk Polytechnic University, Tomsk, Russia, e-mail: malyshev@tpu.ru. Translated from Izvestiya Vysshikh Uchebnykh Zavedenii, Fizika, No. 10, pp. 41–46, October, 2014. Original article submitted June 17, 2014.

The influence of the microstructure on the magnetic characteristics studied in [4] has demonstrated that this dependence is determined mainly by the two factors – porosity and grain sizes. This is due to the fact that the processes of sintering responsible for quantitative and qualitative change of porosity and the recrystallization processes forming the grain structure proceed simultaneously and are interrelated. The grain size in sintered ferrites can influence significantly the ferrite physical and chemical properties. The increased degree of grain size inhomogeneity in the microstructure also causes deterioration of the magnetic characteristics of the material. To suppress the recrystallization process, small additives insoluble in the base material are incorporated into ferrites. Such additives, for example, Bi_2O_3, localized along the grain boundaries form favorable conditions for obtaining high density ferrites with fine-grained ceramic structure at relatively low sintering temperatures [4, 5]. Experimental investigations [6–8] demonstrate that the basic characteristics of the ferrite materials can be changed via the control over their structure due to the application of initial powders with different degrees of dispersion [6] as well as by using different technological methods for producing of such materials [7, 8].

In the present work, we describe a method for controlling over the microstructure formation and the basic electromagnetic characteristics of lithium ferrite ceramics based on $LiFe_5O_8$ by reducing the degree of dispersion of iron oxide used as a basic reagent. We consider iron oxide synthesized by oxidation of ultradisperse iron powders obtained by the electroexplosive method [9]. An analysis of the available data has demonstrated that this approach to the ferrite synthesis has not been used as yet.

EXPERIMENTAL

To synthesize the ultradisperse powder from iron oxide, we used iron nanopowder with particle size of ~100 nm obtained by the electroexplosive method. According to [10] in which the main data on the kinetics and mechanism of oxidation of ultradisperse iron powders obtained by this method were described, heating of α-Fe at temperatures above 600°C caused the formation of nanocrystalline α-Fe_2O_3. In this connection, iron was oxidized in air at a temperature of 700°C for 120 min in a standard resistance-type MPL-6 laboratory furnace (KhimLabo) equipped with a programmable Varta temperature controller. The α-Fe_2O_3 powder so obtained served as an initial reagent for synthesis of lithium ferrite.

Before weighing, initial α-Fe_2O_3 and Li_2CO_3 powders were dried for 3 h at a temperature of ~200°C in a drying oven. The ratio of the initial components of the reaction mixture was calculated from the equation $Li_2CO_3 + 5Fe_2O_3 \rightarrow 2LiFe_5O_8 + CO_2\uparrow$. Iron oxide and lithium carbonate powders were weighed using Shimadzu AUW-D analytical scales with accuracy of ±1 mg in proportion 91.5 mass% iron oxide and 8.5 mass% lithium carbonate.

According to [11], to obtain higher degree of uniformity of the mixture, it was mechanically activated in an AGO-2C planetary mill with the use of steel grinding bowls and balls. Masses of the mixture and balls were in the ratio 1:10, and the treatment time was 15 min. The milling process power was $g = 20$. After mixing, the samples were compacted by single-ended cold pressing into pellets 15 mm in diameter with thickness of 2 mm in a PGr-10 hydraulic press at a constant pressure of 200 MPa for 3 min.

The lithium ferrite samples were synthesized by the ceramic method. Their thermal annealing (synthesis and sintering) was performed in MPL-6 resistance-type furnaces. $LiFe_5O_8$ was synthesized at a temperature of 900°C for 120 min. Then the synthesized powder was subdivided into two parts, and 2 mass% of bismuth trioxide was added to one of the parts to obtain a more dense ceramics. Ferrite ceramics was sintered at a temperature of 1100°C for 120 min. The rates of sample heating and cooling were ~10 deg/min.

The phase composition and the parameters of the crystal lattice of the samples were measured by the method of x-ray diffraction (XRD) analysis using an ARL X'TRA (Switzerland) diffractometer. The XRD patterns were measured using Cu K_α radiation in the range $2\theta = 10–140°$ with a scanning rate of 0.02 deg/s. The phases were identified using the PDF-4 powder database of the International Center for Diffraction Data (ICDD). The XRD patterns were processed by the method of full profile analysis using the *Powder Cell 2.5* software.

Thermogravimetric (TG) and differential scattering calorimetric (DSC) measurements were performed using an STA 449C Jupiter analyzer (Netzsch, Germany) with sensitivity of scales equal to 0.1 μg. The presence of the $LiFe_5O_8$ phase was detected from the Curie temperature by TG measurements in an external magnetic field [12].

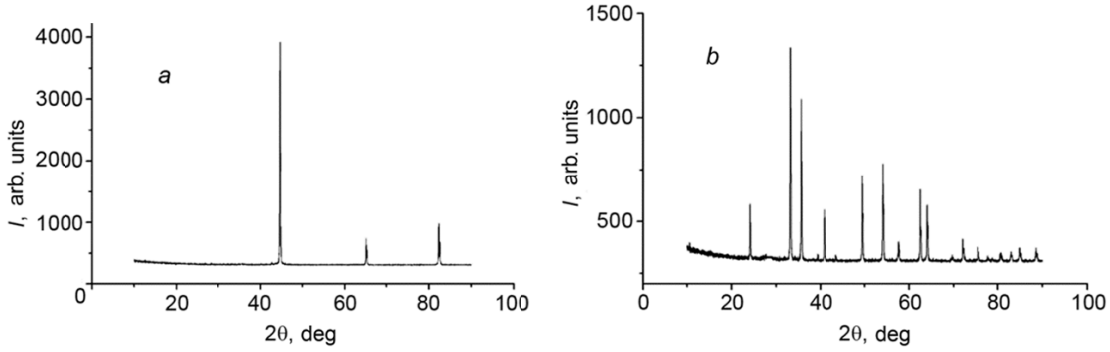

Fig. 1. XRD pattern of iron (*a*) and iron oxide nanopowders (*b*).

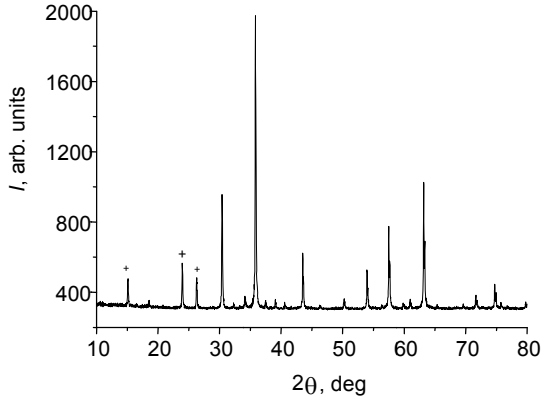

Fig. 2. XRD patterns of synthesised lithium ferrite. Here symbols + indicate superstructure reflections from $LiFe_5O_8$.

The density and the apparent porosity of the samples were determined by the method of hydrostatic weighing using a Shimadzu AUW220D analytical scales. The surface microstructure of the sintered ferrite ceramics was investigated with a Hitachi TM-1000 scanning electron microscope. The spreading resistance method [13] was used to determine the electric conductivity of the ferrite samples. The saturation magnetization was measured in a pulsed magnetic field with amplitude of 5 kOe using an N-04 magnetometer [14].

EXPERIMENTAL RESULTS AND DISCUSSION

Figure 1 shows x-ray diffraction patterns of ultradisperse iron (Fig. 1*a*) and iron oxide powders (Fig. 1*b*) obtained by complete oxidation of iron. According to XRD data, the basic crystal phase of the initial powders was α-Fe, and the final oxidation phase was α-Fe_2O_3. The synthesised samples of lithium ferrite (Fig. 2) are mainly characterized by the presence of the ordered α-$LiFe_5O_8$ phase.

Figures 3 and 4 show the TG/DSC curves for the sintered samples of lithium ferrite ceramics without additives (Fig. 3) and with Bi_2O_3 additive (Fig. 4). The behavior of the TG/DSC curves (Fig. 3) was typical of stoichiometric $LiFe_5O_8$ with high concentration of the ordered α-$LiFe_5O_8$ phase [15]. This conclusion was made based on the following reasons. First, the TG curve shows a mass jump near the Curie temperature equal to ~630°C. This value is close to that of the magnetic transition for $LiFe_5O_8$ [16]. The DSC curve in this region demonstrates the magnetocalorimetric effect corresponding to the magnetic-paramagnetic transition.

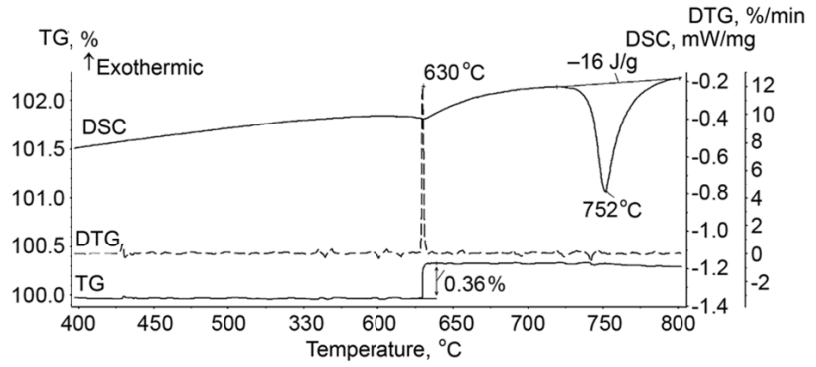

Fig. 3. TG/DSC curves for the $LiFe_5O_8$ lithium ferrite ceramics after sintering.

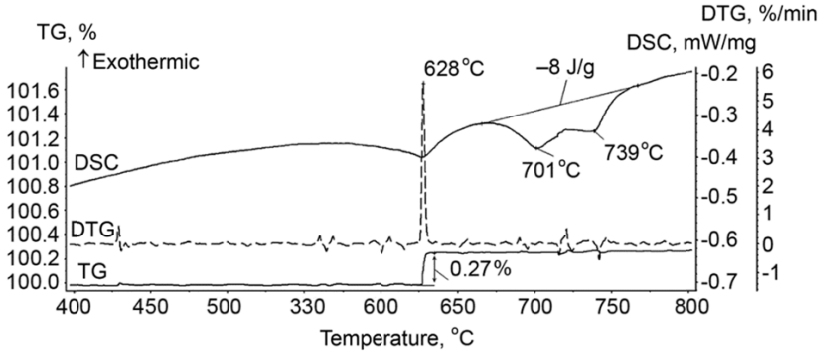

Fig. 4. TG/DSC curves for the $LiFe_5O_8$ lithium ferrite ceramics with Bi_2O_3 additive.

Second, the more intensive high-temperature peak at 752°C (see Fig. 3) is associated with the phase transition of the ordered $LiFe_5O_8$ structure to a disordered state (the so-called $\alpha \rightarrow \beta$ phase transition). The enthalpy of the $\alpha \rightarrow \beta$ transition characterizes the degree of ordering of the lithium spinel structure. It should be noted that the given phase transition is reversible. Upon cooling, the inverse $\beta \rightarrow \alpha$ transition is observed accompanied by an exothermic peak on the DSC curve.

Lithium ferrite samples sintered with Bi_2O_3 additive (Fig. 4) also have high Curie temperature equal to 628°C. However, the DSC curve shows a wide double peak with weak thermal effect. Since lithium ferrite and bismuth trioxide form systems of eutectic type with fusion temperature of ~700°C [4], the double endothermic peak on the DSC curve observed at 670–760°C is due to the superimposed thermal effects corresponding to fusion of the Bi_2O_3 additive during heating and the $\alpha \rightarrow \beta$ transition of the $LiFe_5O_8$ phase.

Figure 5*a* shows the photomicrograph of ferrite samples without Bi_2O_3 additive. It can be seen that these samples have fine-grained polycrystalline structure with average grain size of ~1.4 μm. Somewhat different pictures are observed for the lithium ferrite samples comprising bismuth microcomponent in their composition (Fig. 5*b*). In this case, the ferrite ceramics has larger average grain size of ~4.6 μm. It also can be seen that the Bi_2O_3 additive is distributed along the grain boundaries.

Results of determination of the specific electrical resistance (ρ) demonstrated that the samples of lithium ferrite ceramics were characterized by inhomogeneous distribution of properties with the sample thickness. After sintering the samples acquired surface layers with thickness of the order of 100–200 μm and increased specific electrical resistance formed in the stage of cooling after sintering of the ferrite ceramics [17]. After sanding of these layers, the electrical resistance remained unchanged with the depth. Values of ρ for all examined samples are given in Table 1. The measured values of all basic structural and electromagnetic parameters for the examined samples and samples of the

TABLE 1

Sample type	Average grain size, μm	Density, g/cm^3	Porosity, %	Curie temperature, °C	ρ at T = 20°C, Ω·cm	Saturation magnetization $4\pi M_s$, G
$LiFe_5O_8$	1.4	4.2	9.2	630	$1.0 \cdot 10^7$	3350
$LiFe_5O_8 + Bi_2O_3$	4.6	4.4	4.9	628	$1.0 \cdot 10^4$	3400
$LiFe_5O_8 + Bi_2O_3$ [8, 18]	12	4.4	5.9	629	$3.2 \cdot 10^2$	2800

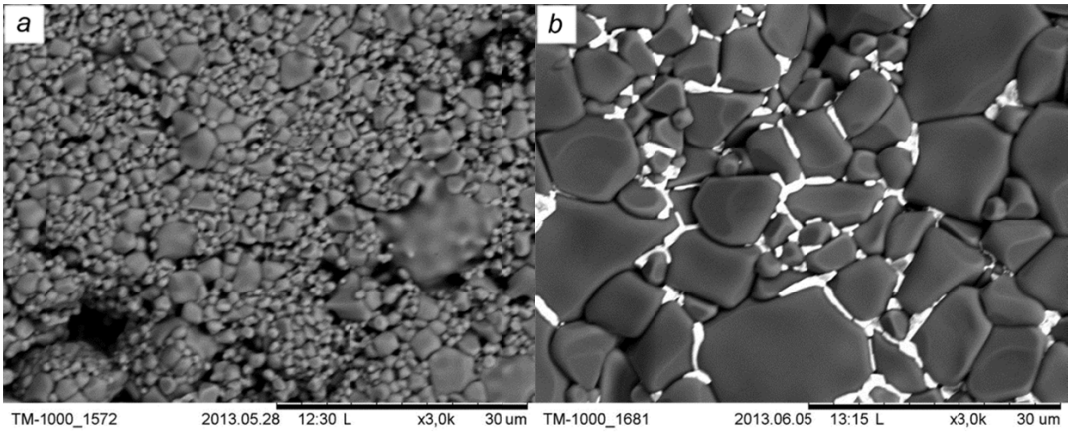

Fig. 5. Microstructure of the lithium ferrite ceramics without (*a*) and with Bi_2O_3 additive (*b*).

same composition synthesized in [8, 18] from the iron oxide powder with average particle sizes 1–10 μm are also presented in Table 1.

From the data presented in Table 1 it follows that the examined samples of lithium ferrite ceramics have high values of the electrical resistance and saturation magnetization. The lithium ferrite samples with bismuth oxide additive demonstrated higher magnetization. However, lower values of the specific electrical resistance are characteristic for them due to larger average grain sizes and lower degrees of porosity. They also possessed higher density in comparison with the samples without bismuth oxide additives.

Comparing the characteristics of the examined samples of ferrite ceramics with those of samples of ceramics possessing the same structure but synthesized from the micron iron oxide powder, we can conclude that the ceramics examined in the present work possesses higher basic electromagnetic characteristics required for microwave magnetic materials [4, 19].

CONCLUSIONS

The structural, magnetic, and electrical characteristics of the lithium ferrite ceramics of $LiFe_5O_8$ composition synthesized from the ultradisperse iron oxide powder have been investigated. The analysis of the set of the results obtained demonstrated the following:

– Examined samples were largely characterized by the presence of the ordered α-$LiFe_5O_8$ phase. The Curie temperature was equal to ~630°C.

– $LiFe_5O_8$ without additives sintered by the ceramic technology were characterized by fine-grained structure with high values of the density, specific electrical resistance, and saturation magnetization that improved its properties (low dielectric and magnetic losses) in the microwave range.

– Lithium ferrite sintered with addition of bismuth oxide was characterized by higher values of the density and average grain size. Lower values of the specific electrical resistance and relatively high values of saturation magnetization were characteristic for such samples. This suggests that such lithium ferrites can be used for the development of coatings interacting efficiently with electromagnetic microwave radiation for which high values of saturation magnetization and large magnetic and dielectric losses are characteristic.

This work was supported in part by the Ministry of Education and Science of the Russian Federation under the State Assignment "Science."

REFERENCES

1. Q. Zhang, J. Song, and L. Wang, Lithium-zinc-ferrite microwave electromagnetic consumable material and preparation method thereof, China Patent No. 101696106 (2010).
2. A. Ahniyaz, T. Fujiwara, S.-W. Song, *et al*., J. Solid State Ionics, **151**, 419–423 (2002).
3. N. Rezlescu, C. Doroftei, E. Rezlescu, *et al*., Sens. Actuators, **B133**, 420–425 (2008).
4. B. E. Levin, Yu. D. Tret'yakov, and L. M. Letyuk, Physical and Chemical Principles of Manufacturing and Property and Application of Ferrites [in Russian], Metallurgiya, Moscow (1979).
5. R. Guo, Z. Yu, Y. Yang, *et al*., J. Alloys Compounds, **589**, 1–4 (2014).
6. U. Topal, J. Magn. Magn. Mater., **320**, 331–335 (2008).
7. V. Babu and P. Padaikathan, J. Magn. Magn. Mater., **241**, 85–88 (2002).
8. A. P. Surzhikov, A. M. Pritulov, E. N. Lysenko, *et al*., J. Thermal Analysis Calorimetry, **110**, 733–738 (2012).
9. N. A. Yavorovskii, Izv. Vyssh. Uchebn. Zaved. Fiz., **37**, No. 4, 114–136 (1994).
10. E. N. Lysenko, A. P. Surzhikov, S. P. Zhuravkov, *et al*., J. Thermal Analysis Calorimetry, **115**, 1447–1452 (2014).
11. A. P. Surzhikov, E. N. Lysenko, A. V. Malyshev, et al., Russ. Phys. J., **55**, No. 6, 672–677 (2012).
12. A. P. Surzhikov, A. M. Pritulov, E. N. Lysenko, *et al*., J. Thermal Analysis Calorimetry, **109**, No. 1, 63–67 (2012).
13. L. P. Pavlov, Methods of Measuring the Parameters of Semiconductor Materials [in Russian], Vysshaya Shkola, Moscow (1987).
14. V. Yu. Kreslin and E. P. Naiden, Prib. Tekh. Eksp., No. 1, 63–66 (2002).
15. A. P. Surzhikov, T. S. Franguljyan, E. N. Lysenko, *et al*., J. Thermal Analysis Calorimetry, **108**, No. 3, 1207–1212 (2012).
16. A. P. Surzhikov, E. N. Lysenko, V. A. Vlasov, *et al*., J. Thermal Analysis Calorimetry, **112**, No. 2, 739–745 (2013).
17. S. A. Gyngazov, E. N. Lysenko, M. S. Petyukevich, and T. S. Frangulyan, Russ. Phys. J., **50,** No. 2, 134–139 (2007).
18. A. P. Surzhikov, T. S. Frangulyan, S. A. Gyngazov, *et al*., Russ. Phys. J., **49**, No. 5, 506–510 (2006).
19. P. D. Baba, G. M. Argentina, W. E. Courtney, *et al*., IEEE Trans Magn., **8**, 83–94 (1972).